

Beyond 7-Azaindole: Conjugation Effects on Intermolecular Double Hydrogen-Atom Transfer Reactions

Carlos R. Baiz, Sarah J. Ledford, Kevin J. Kubarych, and Barry D. Dunietz

J. Phys. Chem. A, **Article ASAP** • DOI: 10.1021/jp8098472 • Publication Date (Web): 30 March 2009

Downloaded from <http://pubs.acs.org> on March 30, 2009

More About This Article

Additional resources and features associated with this article are available within the HTML version:

- Supporting Information
- Access to high resolution figures
- Links to articles and content related to this article
- Copyright permission to reproduce figures and/or text from this article

[View the Full Text HTML](#)

Beyond 7-Azaindole: Conjugation Effects on Intermolecular Double Hydrogen-Atom Transfer Reactions

Carlos R. Baiz, Sarah J. Ledford, Kevin J. Kubarych, and Barry D. Dunietz*

Department of Chemistry, University of Michigan, Ann Arbor, Michigan 48109-1055

Received: November 8, 2008; Revised Manuscript Received: February 8, 2009

Conjugation effects on the thermodynamics of ground-state and lowest-singlet excited-state double hydrogen-atom transfer reactions in 7-azaindole and related models are studied with *ab initio* electronic structure methods. The results indicate that the extended conjugation of the system has a large effect on the relative energies required for hydrogen-atom transfer. The observed energy differences are mainly attributed to stabilization of the tautomer species by enhancing low-energy resonance structures and by allowing for efficient delocalization of excess charge in the reaction center.

I. Introduction

The study of the electronic structure of extended systems and properties affected by the extended nature has been a focus of exhaustive experimental and computational studies.^{1,2} For example, the relation of the conjugation to hydrogen-atom transfer reaction barriers, which are among the most basic, ubiquitous, and important reactions in nature, has been previously explored.^{3,4} Recently, a large experimental and theoretical effort has been directed toward understanding hydrogen-atom transfer reactions in the ground and excited electronic states in systems such as DNA base pairs.^{5–11} Beginning with the experimental work of Taylor et al.,¹² many studies have used simplified model systems such as 7-azaindole dimers to investigate excited-state tautomerization reactions^{13–20} where ultraviolet photoexcitation favors hydrogen-atom transfer. Several results have been interpreted in the context of biologically relevant systems such as DNA base pairs. Therefore, in order to properly interpret and extend previous results, it is important to understand the role of the extended molecule, namely, the coupled conjugation, on the thermodynamics of these reactions.

Intense debate over the mechanism of these reactions has motivated various theoretical studies as well as multiple experiments; some evidence has been found to support a stepwise^{20–24} mechanism while other evidence indicates that the mechanism is concerted.^{25–30} The interpretation of these mechanistic studies is further complicated since quantum effects, particularly tunneling, should not be neglected.^{31–33} Most of the debate is focused on the excited-state potential energy surface. The heart of this debate stems from the complexity of the proton-transfer reaction coordinate. The reaction coordinate involves low-frequency vibrations that are added to the proton motion between the two nitrogen sites. The time scale of the excited-state hydrogen transfer is set not only by the N–H stretching motions but also by other low-frequency modes. In this report, however, we focus mainly on utilizing model systems to obtain insight into the effects of extended conjugation on the *thermodynamics* of these reactions in the ground and lowest-excited electronic states without special regard to the mechanism.

With the recent development of new ultrafast spectroscopic methods such as infrared echo peak shifts and two-dimensional infrared spectroscopy,^{34–36} it has become possible to directly

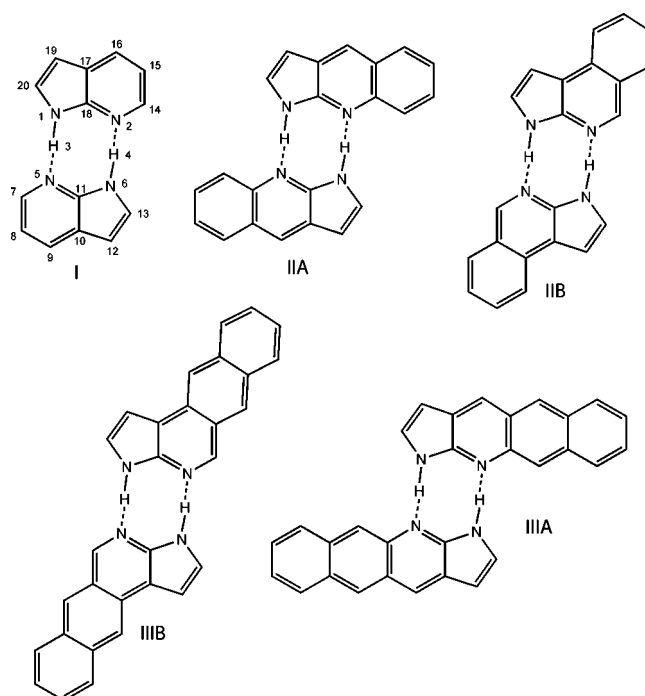


Figure 1. Molecular structures of the five model systems in their normal base-pair (BP) configurations. The atom numbering indicated in model I (7-azaindole C_{2h} dimer) is that used for all models.

observe reaction dynamics, including hydrogen bonding,^{37–39} in real time with femtosecond time resolution. In addition, nonequilibrium multidimensional spectroscopy can follow dynamics induced by photoexcitation^{40,41} and thus offer valuable insight into the mechanisms of hydrogen-atom transfer. We believe that this report will aid in the development of future experiments and the interpretation of the results.

II. Computational Methods and Models

In order to investigate the effects of extended conjugation on hydrogen-atom transfer reactions, we constructed a set of model systems starting with 7-azaindole dimer and then varied the conjugation by adding aromatic rings in two different positions as shown in Figure 1. The models were chosen to test the energetics of hydrogen transfer with regard to the size

* Corresponding author. E-mail: bdunietz@umich.edu.

TABLE 1: Ground- and Excited-State Total Electronic Energies (TE) in Atomic Units, Zero-Point Vibrational Energies (ZPVE) in Atomic Units, and Corresponding Energy Differences (ΔE) between Base-Pair (BP) and Tautomer (TAU) in kJ mol⁻¹ Calculated at the HF/6-31G(d) and CIS/6-31G(d) Levels of Theory^a

model	tautomerization energies					
	ground			excited		
	TE	ZPVE	ΔE	TE	ZPVE	ΔE
I [BP]	-754.956 251 5	0.256 631 93		-754.756 422 5	0.251 926 02	
I [TAU]	-754.920 328 7	0.257 223 15	95.9	-754.763 107 5	0.251 750 73	-18.0
IIA [BP]	-1 060.262 2	0.356 311 68		-1 060.088 501	0.352 471 1	
IIA [TAU]	-1 060.236 1	0.356 998 52	70.1	-1 060.094 403	0.354 007 33	-11.5
IIIA [BP]	-1 365.545 833	0.456 102 98		-1 365.401 814	0.452 263 99	
IIIA [TAU]	-1 365.528 804	0.456 816 91	45.6	-1 365.397 992	0.454 110 98	14.9
IIIB [BP]	-1 060.262 165	0.357 271 02		-1 060.088 479	0.352 649 58	
IIIB [TAU]	-1 060.211 962	0.357 325 21	131.9	-1 060.059 358	0.353 063 92	77.5
IIIB [BP]	-1 365.551 406	0.457 277 46		-1 365.404 84	0.453 282 3	
IIIB [TAU]	-1 365.494 837	0.457 022 48	147.8	-1 365.367 135	0.453 298 24	99.0

^a These data are shown graphically in Figure 2.

of the coupled aromatic system as well as the position of the added rings. Recently, the conjugation effects on the proton transfer of a system with a similar molecular core, azacarbazole, have been studied systematically by experimental means.⁴² We note that the extended conjugated electronic system is coupled in our study to the larger ring of the skeleton, whereas in the azacarbazole the additional conjugated structure is added to the smaller ring. In similar studies, proton-transfer reactions in related systems have been elaborated by analyzing the basicity–acidity of the proton acceptor–donor sites.⁴³ In all the systems detailed below, the two sites are only coupled by hydrogen-bonding interactions. The change in proton-transfer energy due to the varied conjugation is discussed in detail below.

Structure optimizations and harmonic frequency analyses in the ground state were performed using spin-restricted Hartree–Fock theory with the 6-31G(d) Pople basis set. Excited-state geometries were optimized starting from the corresponding ground-state geometries using the configuration interaction single-excitations (CIS) method⁴⁴ with the corresponding Hartree–Fock reference ground state. We note that the use of optimized structures at the density functional theory (DFT) level and the extension of the basis set to use polarizing basis function (6-31++g(d,p)) have not changed significantly the energetic differences as reported below. For example, upon using the larger basis set, the ground-state tautomerization energies only decreased by 3–6 kJ/mol, which is much smaller than the observed energy differences between the different models. Therefore, our analysis of the energetic trends due to the extended conjugation remains unaffected by the addition of polarization functions. Additionally, a DFT-based level [B3LYP/6-31++G(d,p)] yields similar ground-state results, where, although the DFT energy differences are about 60% smaller than those of Hartree–Fock, the observed trends remain unchanged. The trends in excited-state energies are also reproduced by computing the vertical excitations via time-dependent DFT with the corresponding ground-state geometries.

All geometries were optimized in the lowest singlet excited-state corresponding to a ${}^1\pi\pi^*$ excitation. This particular state was chosen as it is the lowest state that leads to tautomerization in 7-azaindole. This excitation predominantly involves the highest occupied and lowest unoccupied molecular orbitals in all the model systems considered. Equilibrium structures exhibit no imaginary frequencies, indicating true minima in the potential energy surface. All computations were performed using the Q-Chem 3.1 package of programs.⁴⁵

The degree of conjugation was measured by computing a generalized nonconjugation index ξ , which is defined as the

difference in length between longest and shortest pyridinic C–N bonds. A small value of ξ corresponds to a conjugated system, whereas a large value represents a system with alternating single and double bonds corresponding to a specific resonance structure. We note that we analyze the dimer interactions at the different structural minima of the different models by following the N–H bond lengths and by population analysis of the different models. As discussed above, however, the reaction mechanism is complex and may involve additional structural features beyond the evolving distances of the transferred proton between the two nitrogen sites.

To ensure that the observed changes in tautomerization energy are due to orbital delocalization and not simple constraints in the carbon–carbon bond lengths imposed by the added rings, we constrained the bonds C₈–C₉, C₁₅–C₁₆, and C₇–C₈, C₁₄–C₁₅ (namely, fixing the backbone geometry) in model **I** to the equilibrium ground- and excited-state carbon–carbon bond lengths in the benzene molecule. No appreciable changes in tautomerization energies were observed, confirming that the differences in energy observed in our models are a consequence of the changes in electronic structure imposed by the extended conjugation of the system.

III. Results and Discussion

As shown in Table 1, ground-state tautomerization is highly endothermic in all models, ranging from 45.6 kJ mol⁻¹ in model **IIIA** to 147.9 kJ mol⁻¹ in model **IIIB**, while excited-state energies range from -18.0 kJ mol⁻¹ in model **I** to 99.0 kJ mol⁻¹ in model **IIIB**. These results show that the thermodynamics of tautomerization are highly sensitive to the extended conjugation of the system and that model molecules may not accurately capture the reaction energetics observed in larger systems. The results also indicate that the position of the added rings has a significant effect on the relative tautomerization energies in the ground and excited states. Naturally, a decrease in the energy required for tautomerization can be accomplished by either destabilization of the base pair or stabilization of the tautomer. Bond length and Mulliken charge analyses, as detailed below, indicate that the energy differences are mainly due to changes in the electronic structure of the tautomers. We will now discuss these effects in detail pertaining to both the ground and excited electronic states.

A. Ground State. The calculated tautomerization energies of the different models at the ground and excited states are provided in Table 1 and Figure 2. It is shown that the addition of a ring in position **A** lowers the energy required for

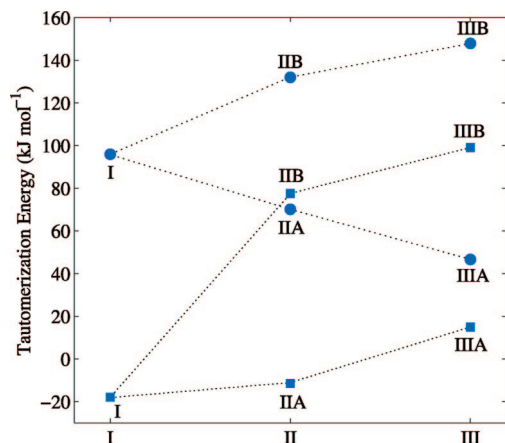


Figure 2. Tautomerization energies for our model systems in the ground (circles) and excited (squares) electronic states. The plot shows a similar trend in the ground and excited states (i.e., addition of a ring in the **B** position raises the energy required for tautomerization). Dashed lines serve only to guide the eye and do not indicate continuity.

tautomerization by 26 kJ mol^{-1} while a ring addition in position **B** increases this energy by 36 kJ mol^{-1} relative to 7-azaindole. Adding a second ring further follows the corresponding trend of the tautomerization.

Analyzing the N–H bond (illustrated in Figure 3) indicates that a ring added in position **A** tends to stabilize the tautomer but does not have a large effect on the stability of the base pair. The N–H bond lengths remain relatively constant in the base pair, indicated by a standard deviation of $7.7 \times 10^{-4} \text{ \AA}$ (models **I–III**); the same analysis in the tautomeric conformations shows a standard deviation of $1.5 \times 10^{-2} \text{ \AA}$, indicating a larger change in bond strength. The same analysis for bond lengths ($\text{N}_2\text{–H}_4$, $\text{N}_5\text{–H}_3$) shows that these bonds are little affected by conjugation in the base pair but exhibit larger variations in the tautomer forms. Therefore, energy differences are mainly due to stabilization of the tautomer relative to the base pair. Furthermore, Figure 3 shows that attaching a ring in position **A** lengthens the N–H bonds in the base pair and shortens them in the tautomer. The addition of a ring in this position slightly destabilizes the base pair while stabilizing the tautomer. These observations are also evident in the ground-state energy trends (Figure 2). Although the tautomerization energy changes are about equal in magnitude for models **IIA–IIIA** and **IIB–IIB** relative to 7-azaindole, the change in bond length is more pronounced in the case of models of the **B** type. It is important to note that the observed changes in bond lengths in systems with different attached conjugation are relatively small overall, but the effect on the energetics of tautomerization is large. This indicates that the position of the added conjugation has large effects on the overall electronic structure of the system whereas the N–H bond lengths are relatively insensitive.

Further insight into the tautomerization process can be obtained by separating the reaction into dimerization (i.e., hydrogen-bonding) and hydrogen-transfer steps. These separate energies are obtained from computing the total energy of each monomer in the normal “base-pair” and “tautomer” conformations and comparing the energies of the monomers to those of the dimers. The results reveal that dimerization energy plays an important role in determining the thermodynamics of the reaction. As expected, dimer formation is more favored in the tautomeric conformation than in the base pair, thus subtracting from the overall endothermicity of the reaction in the ground state. These results are in agreement with the previous observations: lower tautomerization energy, achieved mainly by stabi-

lizing the product, shows stronger N–H bonds in the tautomer conformation, which also correlates to lower dimerization energy and weaker intermolecular hydrogen bonds.

We now analyze the conjugation at the core of the hydrogen-transfer reaction as measured by the nonconjugation coefficient ξ . The corresponding coefficients are provided in Figure 4 for both the base-pair and tautomer forms in the **A** and **B** models. The addition of extra rings decreases the conjugation in the ground state with the base pairs showing a similar coefficient, regardless of the added ring position, and the tautomers showing a more pronounced difference. It is observed that the **A** models exhibit a larger degree of conjugation than the **B** models in their respective tautomer configurations. The increased conjugation lowers the tautomerization energy by stabilizing the tautomers due to delocalization effects. However, since all larger models exhibit higher conjugation with respect to model **I**, the addition of extra rings enhances one resonance structure. This results in effects that compete with the delocalization that dominates the smaller system.

The localization effect, due to the addition of extra rings, can be concisely described by considering a detailed bond length analysis provided in Figure 5. Two different resonance structures are selected by the addition of a ring in the **A** or **B** position. The position of the added ring enhances the structure corresponding to having a double bond where the ring is attached. Because the most stable resonance structure of models **IIA** and **IIIA** more closely matches that of 7-azaindole, tautomerization energy is lower for these two models. In contrast, models **IIB** and **IIB** enhance the “wrong” resonance structure, and thus tautomerization energy becomes higher for these molecules.

Mulliken charge population analyses (Figure 6) reveal that, in the tautomer conformation, models **IIA** and **IIIA** lead to a larger negative charge on the reaction center. A ring attached to the **A** position increases the ability for charge delocalization, which reduces the buildup of charge on N_2 and N_5 , thus stabilizing the tautomer conformation partially by strengthening the $\text{N}_2\text{–H}_4$ and $\text{N}_5\text{–H}_1$ bonds.

To further highlight the difference in the schemes for adding a ring on delocalization of charge, we consider several simplified model molecules. These simplified systems, illustrated in Figure 7, represent monomers **I**, **IIA**, and **IIB** in the tautomeric configuration with the five-membered pyrrole ring removed. The reduced models exhibit the same behavior as the larger systems. Namely, the rings added in scheme **A** couple more efficiently to the central N atom, delocalizing the positive charge on the nitrogen atom more effectively and thus strengthening the N–H bond. Rings added through scheme **B** are, however, less effective in their coupling to the core, and a dominating resonance structure with the similar charge as the basic model **I** is maintained.

B. Excited State. The nature of the lowest singlet excitation in 7-azaindole, $^1\pi\pi^*$, has been previously analyzed in detail.^{18,33} Briefly, the excitation is localized in one of the moieties and involves breaking of the C_{2h} symmetry of the dimer, lowering it to a corresponding C_s point group. Bond lengths remain near their ground-state values in the unit that does not participate in the excitation but vary greatly in the unit where the HOMO and LUMO orbitals are localized. Our results indicate that the addition of extra rings does not change the fundamental nature of this excitation. Figure 8 shows the frontier orbitals in models **I** and **II** in their respective base-pair conformations computed at the excited-state geometries.

Vertical excitation energies decrease from 5.0 eV in model **I** to 3.6 eV in models **IIIA** and **IIB** in the base-pair configuration.

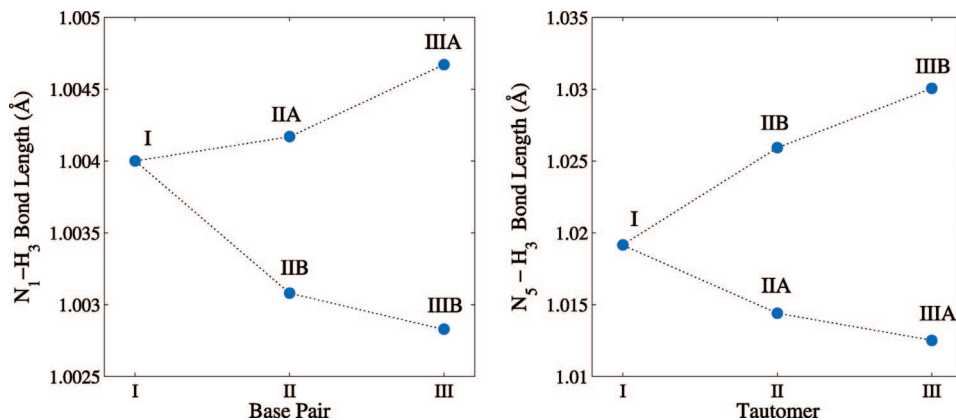


Figure 3. N-H bond lengths for our model systems in the ground state. Lengths corresponding to the base pair are shown in the left plot, and the tautomer lengths are shown in the right plot. Small changes in N-H bond length are observed in the base pairs; these changes become larger in the tautomer conformations. Note the difference in the ordinate scales.

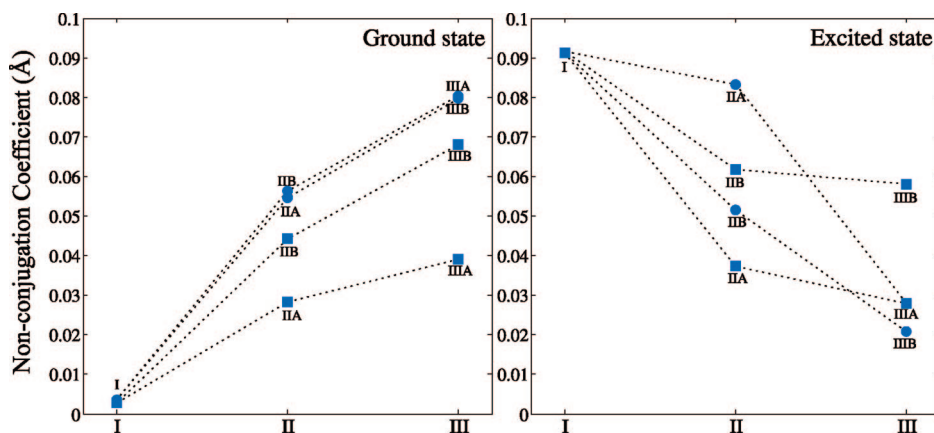


Figure 4. Ground- and excited-state nonconjugation coefficients (ξ) corresponding to the four models in the base-pair (circles) and tautomer (squares) conformations. In the ground state, the coefficient in the base pairs is similar regardless of the position of the added rings while larger deviations are observed in the tautomers. Electronic excitation decreases the conjugation of 7-azaindole; an increase in conjugation for the excited state is seen in the larger models.

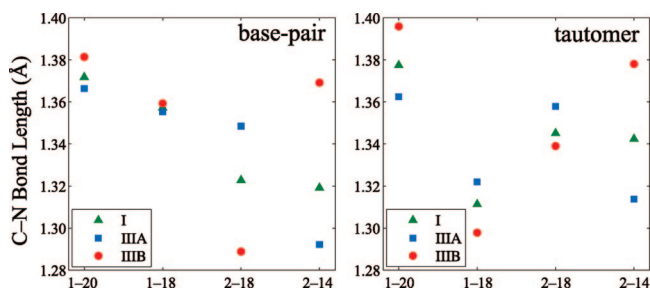


Figure 5. Bond lengths corresponding to the four C-N bonds, N₁-C₂₀, N₁-C₁₈, N₂-C₁₈, and N₂-C₁₄, for the model systems in the ground state. Large deviations are observed in the base-pair and tautomer conformation. The bond-length structure in model **I** is more closely matched by model **IIA**.

Tautomerization also lowers the excitation energy, decreasing from 5.0 to 3.7 eV in model **I**, and from 3.6 to 3.0 eV in model **IIIA**.

Excited-state hydrogen-atom transfer is exothermic only in models **I** and **IIA**, and highly endothermic for models **IIB** and **IIIB** (Table 1). Unlike the ground state, the effect of the added ring on the excited energy levels is to increase the endothermic nature of the reaction. However, the overall energy trend observed in the ground state, namely, that models **IIA** and **IIIA** exhibit lower tautomerization energy than models **IIB** and **IIIB**, is preserved in the excited state as well. This indicates that the effect of coupled conjugation is similar in both ground and

excited states. N-H bond length analyses (not shown) also confirm the observed trends in the excited state. Additionally, the Mulliken charge trends observed in the ground state (Figure 6) are preserved in the excited state.

The differences in tautomerization energies can be understood in terms of the conjugation effects induced by the extra rings. Figure 4 shows that the trends in conjugation are *reversed* in the excited state. Larger systems exhibit lower nonconjugation. Previous studies have shown that in the ground state higher conjugation decreases the barrier for hydrogen transfer, whereas the opposite trend is observed in the excited state: lower conjugation shows a smaller barrier.³ The same behavior is observed for the reaction described here. At the excited state, model **I**, which is the least conjugated, exhibits the lowest tautomerization energy. The assumption that excited-state hydrogen-transfer reactions are indeed stabilized by lower conjugation correctly predicts that the least conjugated system, model **I**, should exhibit the lowest tautomerization energy in the excited state (Table 1). In addition, it is observed that the tautomerization energies in models **A** are overall lower than in models **B** which is evidence that, analogous to the ground state, a lower energy resonance structure is enhanced by the addition of rings in the **A** position.

IV. Conclusion and Summary

Our studies demonstrate that by modifying the resonance structure of 7-azaindole a large effect on the energy required

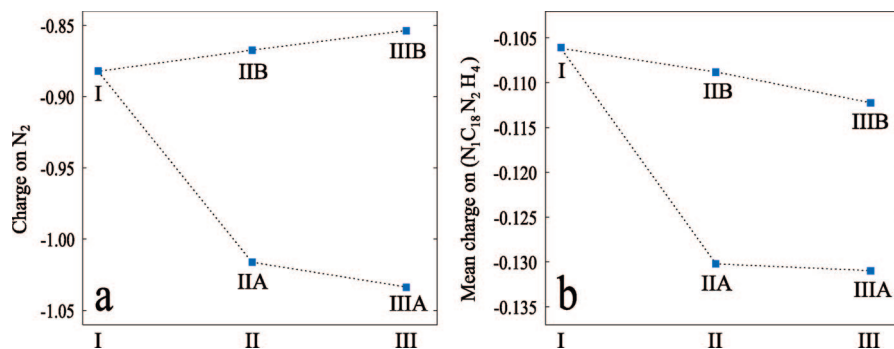


Figure 6. Mean Mulliken charge population on (a) N₂ and N₅ and (b) the main reaction center (N₁, C₁₈, N₂, H₄) for the tautomeric configurations. Similar trends are observed in the base-pair conformations (not shown).

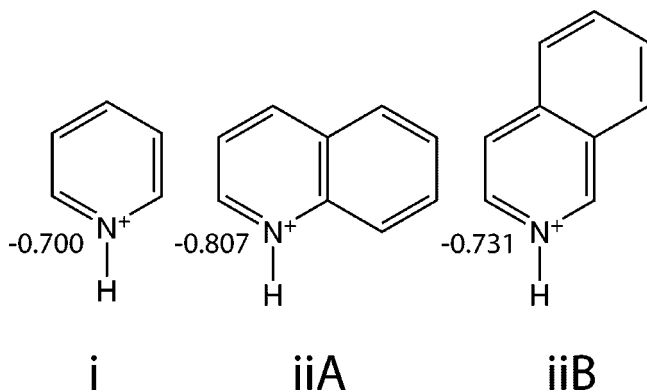


Figure 7. Models i, iiA, iiB, representing the addition of rings in positions A and B in the tautomeric conformations. The figure includes Mulliken charges on the nitrogen atoms. These models were studied in the ground state (singlet, positive charge), at the level of theory described in the methods section. In this configuration a formal positive charge can be assigned to the nitrogen atom.

for tautomerization is observed in the ground and $^1\pi\pi^*$ excited electronic states. Furthermore, the conjugation effect is highly dependent on the structural aspects of coupling the extended conjugated system to the core region. We show that the additional rings in positions A or B lead to qualitatively different tautomerization energies. This different effect on the conjugation of the system can be understood as reflecting stabilizing of different resonance structures. These effects are noted in N–H bond lengths, dimerization energies, C–N bond analysis, and Mulliken charges near the reaction center.

We find that electronic excitation causes an increase in acidity at the pyrrolic site and corresponding increase in basicity at the pyridinic site, clearly explaining the observed decrease in tautomerization energy relative to the ground state in all our model systems. This is in agreement with previous studies by Catalan.⁴³ At the ground state, the trends of the tautomerization energies are opposite with respect to adding the conjugation in the two positions. The reaction becomes less endothermic with the increase in the coupled conjugation along position A and more endothermic for the other site. At the excited state, this dependence is still overall noted, however, with additional aspects due to the nature of the excited state. It is shown that for both series (A and B) the reaction becomes more endothermic at the excited-state level upon extending the conjugation.

Most importantly, our calculations demonstrate that the effect of conjugation can inhibit the hydrogen-transfer reaction at both the ground and excited states. In all the models considered, the geometrical features of the reaction core remain very similar, indicating that the energetic effects are purely due to electronic conjugation effects. This effect can be exploited by experimen-

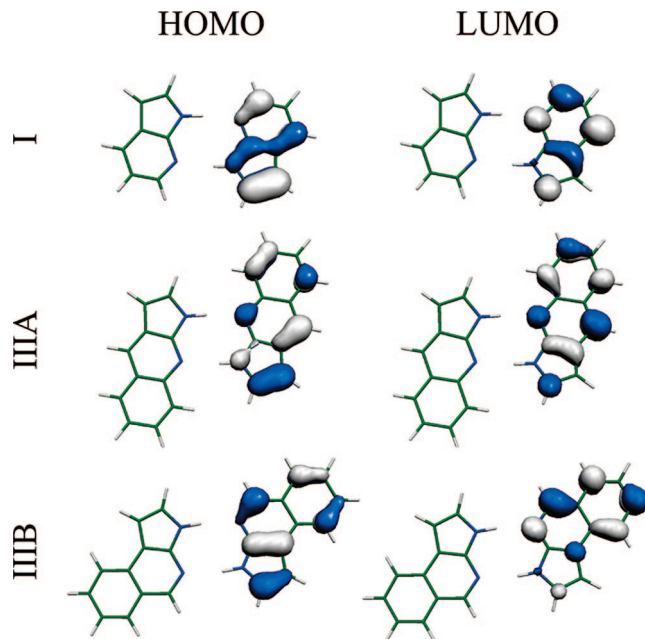


Figure 8. HOMO and LUMO orbitals involved in the $\pi\pi^*$ transitions in models I, IIIA, and IIIB in the base-pair conformation showing a large increase in electron density on N₂ and N₅ upon excitation. The corresponding orbitals in the tautomeric configuration (not shown) exhibit no qualitative difference.

talists aiming to decouple excitations from hydrogen-atom transfer processes in DNA analogs and yields new insight into the mechanism of these reactions. Additionally, it may be possible to control the tautomerization energy and the respective reaction barriers by constructing systems with specific resonance structures and by employing mixed base pairs where the conjugation of each base is different.

Acknowledgment. B.D.D. acknowledges the University of Michigan for support.

References and Notes

- (1) Lange, A. W.; Rohrdanz, M. A.; Herbert, J. M. *J. Phys. Chem. B* **2008**, *112*, 6304–6308.
- (2) Smith, S. M.; Li, X.; Markevitch, A.; Romanov, D.; Levis, R. J.; Schlegel, H. B. *J. Phys. Chem. A* **2007**, *111*, 6920–6932.
- (3) Baiz, C. R.; Dunietz, B. D. *J. Phys. Chem. A* **2007**, *111*, 10139–10143.
- (4) Kong, L.; Priyadarsini, K. I.; Zhang, H. Y. *J. Mol. Struct.—Theochem* **2004**, *684*, 111–116.
- (5) Douhal, A.; Lahmani, F.; Zewail, A. H. *Chem. Phys.* **1996**, *207*, 477–498.
- (6) Scheiner, S. *J. Phys. Chem. A* **2000**, *104*, 5898–5909.

- (7) Gorb, L.; Podolyan, Y.; Dziekonski, P.; Sokalski, W. A.; Leszczynski, J. *J. Am. Chem. Soc.* **2004**, *126*, 10119–10129.
- (8) Zhang, J. D.; Chen, Z.; Schaefer, H. F. *J. Phys. Chem. A* **2008**, *112*, 6217–6226.
- (9) Gu, J.; Xie, Y.; Schaefer, H. F. *J. Chem Phys.* **2007**, *127*, 155107.
- (10) Kim, S.; Meehan, T.; Schaefer, H. F. *J. Phys. Chem. A* **2007**, *111*, 6806–6812.
- (11) Lind, M. C.; Richardson, N. A.; Wheeler, S. E.; Schaefer, H. F. *J. Phys. Chem. B* **2007**, *111*, 5525–5530.
- (12) Taylor, C. A.; El-Bayoumi, M. A.; Kasha, M. *Proc. Natl. Acad. Sci.* **1969**, *63*, 253–260.
- (13) Chachisvilis, M.; Fiebig, T.; Douhal, A.; Zewail, A. H. *J. Phys. Chem. A* **1998**, *102*, 669–673.
- (14) Catalan, J.; de Paz, J. L. G. *J. Chem Phys.* **2005**, *123*, 114302.
- (15) Catalán, J.; de Paz, J. L. G. *J. Chem Phys.* **2005**, *122*, 244320.
- (16) Sakota, K.; Okabe, C.; Nishi, N.; Sekiya, H. *J. Phys. Chem. A* **2005**, *109*, 5245–5247.
- (17) Gelabert, R.; Moreno, M.; Lluch, J. *J. Phys. Chem. A* **2006**, *110*, 1145–1151.
- (18) Serrano-Andres, L.; Merchan, M. *Chem. Phys. Lett.* **2006**, *418*, 569–575.
- (19) Dwyer, J. R.; Dreyer, J.; Nibbering, E. T. J.; Elsaesser, T. *Chem. Phys. Lett.* **2006**, *432*, 146–151.
- (20) Moreno, M.; Douhal, A.; Lluch, J. M.; Castano, O.; Frutos, L. M. *J. Phys. Chem. A* **2001**, *105*, 3887–3893.
- (21) Douhal, A.; Kim, S. K.; Zewail, A. H. *Nature* **1995**, *378*, 260–263.
- (22) Kwon, O.-H.; Zewail, A. H. *Proc. Natl. Acad. Sci.* **2007**, *104*, 8703–8708.
- (23) Hsieh, W.-T.; Hsieh, C.-C.; Lai, C.-H.; Cheng, Y.-M.; Ho, M.-L.; Wang, K. K.; Lee, G.-H.; Chou, P.-T. *Chem. Phys. Chem.* **2008**, *9*, 293–299.
- (24) Zewail, A. H.; Kwon, O.-H. *Proc. Natl. Acad. Sci. U.S.A.* **2008**, *105*, E79.
- (25) Catalan, J.; Valle, J. C. d.; Kasha, M. *Proc. Natl. Acad. Sci. U.S.A.* **1999**, *96*, 8338–8343.
- (26) Takeuchi, S.; Tahara, T. *Chem. Phys. Lett.* **1997**, *277*, 340–346.
- (27) Takeuchi, S.; Tahara, T. *Chem. Phys. Lett.* **2001**, *347*, 108–114.
- (28) Takeuchi, S.; Tahara, T. *Proc. Natl. Acad. Sci.* **2007**, *104*, 5285–5290.
- (29) Catalan, J.; Perez, P.; Del Valle, J. C.; De Paz, J. L. G.; Kasha, M. *Proc. Natl. Acad. Sci. U.S.A.* **2004**, *101*, 419–422.
- (30) Catalan, J. *Proc. Natl. Acad. Sci. U.S.A.* **2008**, *105*, E79.
- (31) Sekiya, H.; Sakota, K. *Bull. Chem. Soc. Jpn.* **2006**, *79*, 373–385.
- (32) Catalan, J.; Kasha, M. *J. Phys. Chem. A* **2000**, *104*, 10812–10820.
- (33) Sekiya, H.; Sakota, K. *J. Photochem. Photobiol., C* **2008**, *9*, 81–91.
- (34) Cho, M. *Chem. Rev.* **2008**, *108*, 1331–1418.
- (35) Jonas, D. M. *Annu. Rev. Phys. Chem.* **2003**, *54*, 425–463.
- (36) Khalil, M.; Demirdoven, N.; Tokmakoff, A. *J. Phys. Chem. A* **2003**, *107*, 5258–5279.
- (37) Kolano, C.; Helbing, J.; Kozinski, M.; Sander, W.; Hamm, P. *Nature* **2006**, *444*, 469–72.
- (38) Zheng, J. R.; Kwak, K.; Asbury, J.; Chen, X.; Piletic, I. R.; Fayer, M. D. *Science* **2005**, *309*, 1338–1343.
- (39) Petersen, P. B.; Roberts, S. T.; Ramasesha, K.; Nocera, D. G.; Tokmakoff, A. *J. Phys. Chem. B* **2008**, *112*, pp 13167.
- (40) Hamm, P.; Helbing, J.; Bredenbeck, J. *Annu. Rev. Phys. Chem.* **2008**, *59*, 291–317.
- (41) Baiz, C. R.; Nee, M. J.; McCanne, R.; Kubarych, K. J. *Opt. Lett.* **2008**, *33*, 2533–2535.
- (42) Catalan, J. *J. Phys. Chem. A* **2007**, *111*, 8774.
- (43) Catalan, J. *J. Am. Chem. Soc.* **2001**, *123*, 11940.
- (44) Foresman, J. B.; Head-Gordon, M.; Pople, J. A.; Frisch, M. J. *J. Phys. Chem.* **1992**, *96*, 135–149.
- (45) Shao, Y.; et al. *Phys. Chem. Chem. Phys.* **2006**, *8*, 3172–91.